

Equivalent Noise Charge Contribution of the \sqrt{f} Parallel Noise in Nuclear Spectroscopic Measurements Using Different Shaping Amplifiers

Stefano Capra, Giacomo Secci, Alberto Pullia

Abstract—In this work both a theoretical study and experimental measurements are shown to describe the ENC (Equivalent Noise Charge) contribution of the parallel \sqrt{f} noise of a charge-sensitive pre-amplifier in a nuclear spectroscopic chain. Previous works have demonstrated that this noise is produced by the distributed capacitive coupling to bulk of the preamplifiers' high-valued feedback resistors, which give rise to a R-C structure known in literature as "diffusive line". The introduced noise is particularly evident when such devices are integrated in a chip using a polysilicon layer that has intrinsically high distributed capacitance to the chip's bulk. Different shaping amplifiers are taken into consideration (analog quasi-Gaussian, digital trapezoidal/triangular, CR-RCⁿ) and closed-form expressions of noise coefficients are given whenever possible.

Keywords—Diffusive Lines, Distributed Capacitance, Electronic Noise, Nuclear Spectroscopy

I. INTRODUCTION

In nuclear spectroscopy with solid state detectors (silicon [1], [2], High-Purity Germanium - HPGe [3]), the energy deposited by the radiation is converted into free charge carriers that must be collected and measured. This is done by the CSP (Charge-Sensitive Pre-amplifier) that is connected, directly or through a decoupling capacitor, to the detector's electrodes. The concept of spectroscopic resolution is directly connected to the ability of measuring the collected charge with the highest possible precision. All the noise sources in the circuit contribute to different extents to the overall noise of the energy measurement. Being the energy measurement ultimately a charge measurement, the associated error can be expressed in electrons rms or Coulomb rms and is generally referred to with the expression "Equivalent Noise Charge" (ENC). The signal from the pre-amplifiers is then processed with dedicated shaping amplifiers, analog or digital, that have the aim to maximize the signal-to-noise ratio. An extensive literature [4] [5] describes the techniques to minimize the ENC given different kinds of shaping amplifiers, but the typical noise sources that are taken into account don't include the parallel \sqrt{f} noise.

Previous works [6] demonstrate, both theoretically [7] and experimentally [8], that this noise is produced by the feedback resistor when this component is coupled with a distributed

capacitance to a ground plane or other conductor. The physical source of this noise is still the resistor thermal excitation but the non-white spectral density is due to the distributed impedance of the device. In nuclear spectroscopy the value of such component is chosen to be as high as possible in order to minimize the associated parallel white noise and commonly a 1 or 2 G Ω discrete resistor is used. The study of a solution to integrate such a device on an ASIC (Application-Specific Integrated Circuit) leads naturally to evaluate the performance of on-chip polysilicon resistors, intrinsically radio-pure and suitable for low radiation background applications. Although expensive in terms of area, these resistors can be realized with reasonable dimensions thanks to high-resistance polysilicon modules offered by many foundry technologies like AMS. Considering the technology AMS C35, a 350 nm CMOS process well suited for analog, low-noise [9] [10] low-power [11] [12] applications, a 100 M Ω resistor is coupled to bulk or to the underlying n-wells with roughly 10 pF of distributed capacitance. As explained and experimentally confirmed in [6], the device, connected as a feedback resistor in a charge-sensitive pre-amplifier, is a current noise source whose Power Spectral Density (PSD) is:

$$PSD(\omega) = \frac{2KT}{R} \sqrt{|\omega| \frac{RC}{2}} \cdot \left[\frac{\sin\left(2\sqrt{|\omega| \frac{RC}{2}}\right) + \sinh\left(2\sqrt{|\omega| \frac{RC}{2}}\right)}{\cosh\left(2\sqrt{|\omega| \frac{RC}{2}}\right) - \cos\left(2\sqrt{|\omega| \frac{RC}{2}}\right)} \right] \quad (1)$$

where R is the total resistance and C is the total stray capacitance of the Resistance With Distributed Capacitance (RWDC). We will refer to this capacitance from now on with the acronym C_{RWDC} . The power spectrum in (1) can be simplified as the sum of two uncorrelated components: a white one (PSD_{white}) and a colored one ($PSD_{\sqrt{f}}$):

$$PSD_{white} = \frac{2kT}{R} \quad (2)$$

$$PSD_{\sqrt{f}}(\omega) = \frac{2kT}{R} \sqrt{|\omega| \frac{RC_{RWDC}}{2}} = \frac{2kT}{R} \sqrt{|\omega| \tau_{RWDC}} \quad (3)$$

Throughout this document the PSD expressions are bilateral and should be integrated from $-\infty$ to $+\infty$ to obtain the variance of the variable they are referred to. We can define, as explained in [6], a noise corner frequency as the frequency where PSD_{white} and $PSD_{\sqrt{f}}$ become equal:

$$f_{CORNER} = \frac{1}{2\pi \left(\frac{RC_{RWDC}}{2} \right)} = \frac{1}{2\pi \tau_{RWDC}} \quad (4)$$

S. Capra is with the Department of Physics, University of Milano and INFN of Milano, Italy (email: stefano.capra@unimi.it).

G. Secci is with the Department of Physics, University of Milano and INFN of Milano, Italy

A. Pullia is with the Department of Physics, University of Milano and INFN of Milano, Italy

In the following sections we will calculate the ENC contributions of the \sqrt{f} parallel noise source using trapezoidal, triangular, quasi-Gaussian and CR-RCⁿ shaping amplifiers.

II. DEFINITION OF THE SYSTEM UNDER STUDY

We will focus on a simplified spectroscopic chain represented in Fig. 1. The pre-amplifier and the shaping amplifier are modeled by a single block with transfer function $S(f)$. $S(f)$ is the product of the transfer function of the pre-amplifier and that of the shaping amplifier, which is indicated as $H(f)$ in Fig. 1. The white series noise of the pre-amplifier input stage is represented by $v_{1/f}^2$ and the series 1/f noise is represented by v_{white}^2 . The i_{white}^2 noise generator is the sum of the shot noise of the detector, i_{shot}^2 , and the shot noise of the input transistor gate current, i_{si}^2 . The i_{RWDC}^2 noise generator represents the white (2) and non-white (3) components of the RWDC noise: this is the noise source this work is focused on. The capacitor C_{TOT} represents the sum of all the capacitances of the system: detector capacitance, feedback capacitance, input transistor capacitance and all the other stray capacitances referred to the input node. The expression of the equivalent input-referred power spectral density of current noise is:

$$PSD_{IN}(f) = a + b \cdot |f| + c \cdot f^2 + PSD_{RWDC}(f), \quad (5)$$

where

$$PSD_{RWDC}(f) = \begin{cases} a' & f \leq f_{CORNER} \\ d \cdot \sqrt{|f|} & f > f_{CORNER} \end{cases} \quad (6)$$

The following formulas represent the explicit definitions of the coefficients a , a' , b , c and d in (5) and (6).

$$a = q_e I_{DET} + q_e I_{FET}, \quad a' = 2kT/R_F \quad (7)$$

$$b = A_f \cdot (2\pi \cdot C_{TOT})^2, \quad \text{with} \quad v_{1/f}^2 = \frac{A_f}{|f|} \quad (8)$$

$$c = \frac{2kT\gamma}{g_m} (2\pi \cdot C_{TOT})^2 \quad (9)$$

$$d = \frac{2kT}{R_F} \sqrt{2\pi\tau_{RWDC}} \quad (10)$$

In these formulas q_e is the electron charge, g_m is the input transistor trans-conductance and γ is the channel thermal noise coefficient for the input device. In this way all the noise sources of the circuit are written as noise current generators referred to the input of a trans-impedance block with transfer function $S(f)$ and zero input impedance. $S(f)$ is the Fourier transform of the spectroscopic chain impulse response $s(t)$. The equivalent noise charge of the spectroscopic chain, expressed in [C]², is calculated with the following equation,

$$\begin{aligned} ENC^2 = & \int_{-\infty}^{+\infty} df \cdot (a + b \cdot |f| + c \cdot f^2) \cdot \left| \frac{S(f)}{A_0} \right|^2 + \\ & + \int_{-f_{CORNER}}^{+f_{CORNER}} df \cdot a' \cdot \left| \frac{S(f)}{A_0} \right|^2 + \\ & + \int_{-\infty}^{-f_{CORNER}} df \cdot d \cdot \sqrt{|f|} \cdot \left| \frac{S(f)}{A_0} \right|^2 + \\ & + \int_{f_{CORNER}}^{+\infty} df \cdot d \cdot \sqrt{|f|} \cdot \left| \frac{S(f)}{A_0} \right|^2, \end{aligned} \quad (11)$$

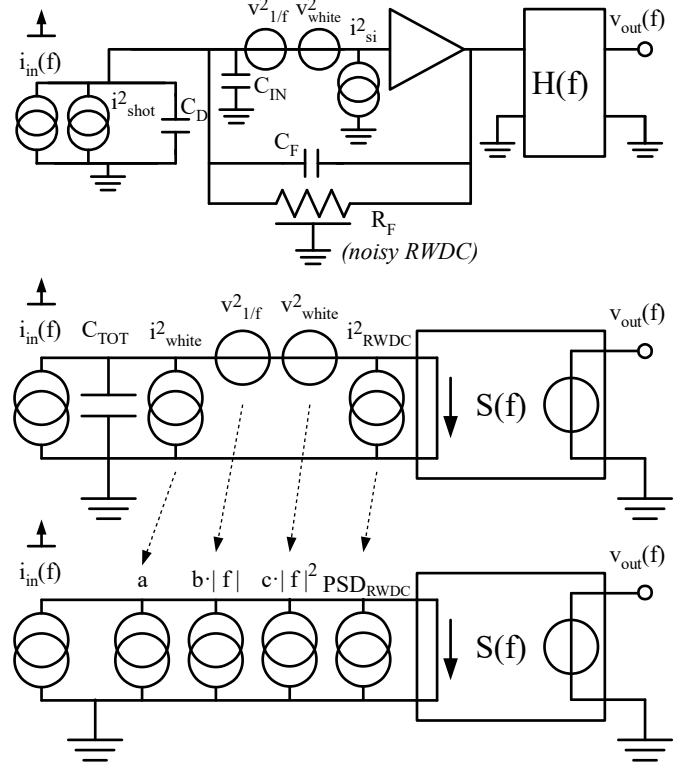


Fig. 1. *Upper figure:* Schematic diagram of a charge-sensitive preamplifier with its noise sources. The feedback resistance is a noisy RWDC. The preamp is followed by a generic shaping amplifier with transfer function $H(\omega)$. *Center figure:* Simplified schematic reporting the typical noise sources in a spectroscopic chain. The pre-amplifier and the shaping amplifier are condensed into a single two-port block with zero input impedance and trans-impedance $S(\omega)$. The detector is represented as a current generator that produces delta-like current signals. *Bottom Figure:* all the noise sources are turned into their Norton equivalent.

which can be rewritten, taking into account that the integrand is an even function, as:

$$\begin{aligned} ENC^2 = & 2 \cdot \int_0^{+\infty} df \cdot (a + b \cdot |f| + c \cdot f^2) \cdot \left| \frac{S(f)}{A_0} \right|^2 + \\ & + 2 \cdot \int_0^{f_{CORNER}} df \cdot a' \cdot \left| \frac{S(f)}{A_0} \right|^2 + \\ & + 2 \cdot \int_{f_{CORNER}}^{+\infty} df \cdot d \cdot \sqrt{|f|} \cdot \left| \frac{S(f)}{A_0} \right|^2, \end{aligned} \quad (12)$$

In (11) and (12) A_0 is the amplitude of $s(t)$, introduced to normalize the transfer function $S(f)$. To correctly evaluate the noise contribution of the resistor with distributed capacitance, we considered its power spectral density white for $f \in (0, f_{CORNER})$ and colored for $f \in (f_{CORNER}, +\infty)$, as described in (2) and (3) respectively. Due to the nature of the integral, it is possible to express (12) in this form:

$$\begin{aligned} ENC^2 = & (a' \cdot K_1 + a) \cdot \tau \cdot \Omega_1 + b \cdot \Omega_2 + \\ & + c \cdot \frac{\Omega_3}{\tau} + d \cdot \sqrt{\tau} \cdot K_4 \cdot \Omega_4, \end{aligned} \quad (13)$$

where the coefficients Ω are reported in table III. Specifically, the expressions for Ω_4 , which is the coefficient related to the

noise component discussed in this work, will be mathematically derived for different shaping amplifiers in the following paragraphs. K_1 and K_4 are weighting coefficients that are functions of τ/τ_{RWDC} , i.e. the ratio between the shaping time of the filter used and the corner time between the white and colored noise of the resistor. The expressions come from the following equations:

$$\int_0^{+f_{CORNER}} df \cdot a \cdot \left| \frac{S(f)}{A_0} \right|^2 = K_1 \cdot \int_0^{+\infty} df \cdot a \cdot \left| \frac{S(f)}{A_0} \right|^2 \quad (14)$$

and

$$\begin{aligned} \int_{f_{CORNER}}^{+\infty} df \cdot d \cdot \sqrt{|f|} \cdot \left| \frac{S(f)}{A_0} \right|^2 &= \\ = K_4 \cdot \int_0^{+\infty} df \cdot d \cdot \sqrt{|f|} \cdot \left| \frac{S(f)}{A_0} \right|^2 & \end{aligned} \quad (15)$$

The physical meaning of K_1 and K_4 is the following: if f_{CORNER} is extremely low with respect to the typical frequencies of a shaping amplifier, the white noise component from the RWDC can be neglected and the \sqrt{f} is dominant. Conversely, if f_{CORNER} is much higher than the typical frequencies of a shaping amplifier, the \sqrt{f} component is to be neglected in favour of the white one. In all the intermediate cases the K_1 and K_4 coefficients mix the two effects in the correct proportion.

In the following sections the exact calculations of the integrals described will be carried out for the most common shaping amplifier types. We define ENC_d^2 as the value of ENC^2 in (13) when the first four components of $PSD_{IN}(f)$ are neglected ($a = a' = b = c = 0$), so that only the $d\sqrt{|f|}$ component is considered, and assuming $K_4 = 1$.

III. TRAPEZOIDAL AND TRIANGULAR SHAPING

The spectroscopic chain made of CSP followed by a trapezoidal filter considered in this section will generate a signal with unitary flat-top height (or tip, in case of triangular shape) in response to a unitary delta-like current signal at the input. We define τ_m the filter risetime and τ_d the length of the flat-top. Such a function $s(t)$ is equivalent to the convolution (represented here with the symbol “ $*$ ”) of two rectangular functions with proper normalization:

$$s(t) = s_1(t) * s_2(t) = \begin{cases} 0 & \text{for } t < 0 \\ \frac{t}{\tau_m} & \text{for } 0 \leq t < \tau_m \\ 1 & \text{for } \tau_m \leq t < \tau_m + \tau_d \\ -\frac{t}{\tau_m} + \frac{2\tau_m + \tau_d}{\tau_m} & \text{for } \tau_m + \tau_d \leq t < 2\tau_m + \tau_d \\ 0 & \text{for } t \geq 2\tau_m + \tau_d \end{cases} \quad (16)$$

with

$$s_1(t) = \begin{cases} 0 & t \leq 0 \\ \frac{1}{\tau_m} & 0 < t \leq \tau_m \\ 0 & t > \tau_m \end{cases} \quad s_2(t) = \begin{cases} 0 & t \leq 0 \\ 1 & 0 < t \leq \alpha\tau_m \\ 0 & t > \alpha\tau_m \end{cases} \quad (17)$$

where $\alpha\tau_m = \tau_m + \tau_d$. Obviously the case with $\alpha = 1$ corresponds to a triangular shaping. We can re-write (12) excluding

all the noise components of PSD_{IN} except $d \cdot \sqrt{|f|}$ and writing the transforms of S_1 and S_2 obtaining:

$$ENC_d^2 = \int_{-\infty}^{+\infty} \frac{d\omega}{2\pi} \cdot \left(d \cdot \sqrt{\frac{|\omega|}{2\pi}} \right) \cdot \left[\frac{\sin(\omega\tau_m/2)}{\omega\tau_m/2} \right]^2 \cdot \left[\alpha\tau_m \frac{\sin(\alpha\omega\tau_m/2)}{\alpha\omega\tau_m/2} \right]^2 \quad (18)$$

We can apply the substitution $x = \omega\tau_m/2$ and, given that the function to be integrated is even, evaluate the integral only between 0 and $+\infty$.

$$ENC_d^2 = \frac{d\sqrt{\tau_m}}{(\pi)^{3/2}} \cdot 2 \int_0^{+\infty} dx \frac{\sin^2(x)\sin^2(\alpha x)}{x^{7/2}} \quad (19)$$

The value of ENC_d^2 is:

$$ENC_d^2 = d \cdot \frac{8\sqrt{\tau_m}}{15\pi} [(\alpha - 1)^{5/2} + (\alpha + 1)^{5/2} - 2(1 + \alpha^{5/2})] \quad (20)$$

and consequently,

$$\Omega_4 = \frac{8}{15\pi} [(\alpha - 1)^{5/2} + (\alpha + 1)^{5/2} - 2(1 + \alpha^{5/2})] \quad (21)$$

The value of the expression in square brackets goes from roughly 1.65 for $\alpha = 1$ to 3.27 for $\alpha = 2$. This means that for $0 < \tau_d < \tau_m$ we can write

$$d\sqrt{\tau_m} \cdot 0.28... < ENC_d^2 < d\sqrt{\tau_m} \cdot 0.56... \quad (22)$$

IV. QUASI-GAUSSIAN SHAPING

Commercial Quasi-Gaussian shaping amplifiers are generally constituted by a fourth-order filter section with additional baseline-restoring circuits [13]. We will not consider the latter and only take into account the frequency response function, reported in (23).

$$S_{QG}(\omega) = \frac{\beta}{(\frac{1}{\tau} + i\omega)(\frac{3}{\tau} + i\omega)(\frac{1-4/5i}{\tau} + i\omega)(\frac{1+4/5i}{\tau} + i\omega)} \quad (23)$$

The constant β is the normalization factor, still to be calculated, that ensures that the filter impulse-response function has unitary amplitude. We will keep $\beta = 1$ at the moment. The impulse-response function of $S_{QG}(\omega)$, $s_{QG}(t)$ can be easily calculated with residue theorem. Its expression is:

$$s_{QG}(t) = \tau^3 \frac{25}{32} e^{-t/\tau} \left[1 - \frac{4}{29} e^{-2t/\tau} - \frac{25}{29} \cos\left(\frac{4t}{5\tau}\right) - \frac{10}{29} \sin\left(\frac{4t}{5\tau}\right) \right] u(t) \quad (24)$$

where $u(t)$ is the Heaviside step function. The maximum amplitude of this pulse can be calculated evaluating the function in (24) in the point where the first derivative is zero. This is equivalent to solving the equation

$$12e^{-\frac{5}{2}x} + 30\sin(x) + 17\cos(x) = 29 \quad (25)$$

where x is:

$$x = \frac{4t}{5\tau} \quad (26)$$

Due to the oscillatory nature of the function, there are infinite solutions including, obviously, the point $t = 0$. The solution we are interested in is for $x \approx 1.6375...$, that means for $t/\tau = 2.0469... \approx 2$. At this point we can calculate the non-normalized filter impulse-response amplitude substituting $t/\tau = 2$ in (24).

$$\max[h_{QG}(t)] = \tau^3 \cdot 0.0717... = \zeta\tau^3 \quad (27)$$

The normalizing factor β reported in (23) is thus equivalent to:

$$\beta = \frac{1}{\zeta \tau^3}. \quad (28)$$

We can now re-write (12) excluding all the noise components except $d \cdot \sqrt{|f|}$.

$$ENC_d^2 = \int_{-\infty}^{+\infty} \frac{d\omega}{2\pi} \cdot d\sqrt{\frac{|\omega|}{2\pi}} \cdot \left| \frac{1/\zeta \tau^2}{(1+i\omega\tau)(3+i\omega\tau)(1+0.8i+i\omega\tau)(1-0.8i+i\omega\tau)} \right|^2 \quad (29)$$

We can simplify this expression evaluating the modulus, putting $x = \omega\tau$ and acknowledging the symmetry of the integral:

$$ENC_d^2 = \frac{d\sqrt{\tau}}{\zeta^2(2\pi)^{3/2}} \cdot 2 \int_0^{+\infty} dx \frac{\sqrt{x}}{(1+x^2)(9+x^2)(1.64+1.6x+x^2)(1.64-1.6x+x^2)} \quad (30)$$

$$ENC_d^2 = \frac{d\sqrt{\tau}}{\zeta^2(2\pi)^{3/2}} \cdot 0.0434364... = d\sqrt{\tau} \cdot 0.5365... \quad (31)$$

The coefficient Ω_4 is given by:

$$\Omega_4 = \frac{1}{\zeta^2(2\pi)^{3/2}} \cdot 0.0434364... = 0.5365... \quad (32)$$

V. CR-RCⁿ SHAPING

A CR-RCⁿ shaper is a cascade of a single-pole high-pass filter followed by n single-pole low-pass stages. By definition this filter is applied to the output of an ideal integrating stage. In reality, being the CSP a non-ideal integrator, the first stage is realized with other circuit solutions like pole-zero networks. The transfer function of such a spectroscopic chain is the following:

$$S_{CR-RC^n} = \frac{1}{j\omega} \cdot \frac{j\omega \cdot \tau}{1+i\omega\tau} \cdot \frac{1}{(1+i\omega\tau)^n}. \quad (33)$$

The time-domain impulse-response $s_{CR-RC^n}(t)$ can be calculated with the residue theorem and is equal to:

$$s_{CR-RC^n}(t) = \frac{\varepsilon}{n!} \left(\frac{t}{\tau} \right)^n e^{-t/\tau} \quad (34)$$

with the normalizing factor $\varepsilon = n!/(n^n \cdot e^{-n})$. Substituting the result of (34) in (12) and considering only the $d\sqrt{|f|}$ term of PSD_{IN} we obtain:

$$ENC_d^2 = \int_{-\infty}^{+\infty} \frac{d\omega}{2\pi} \cdot d\sqrt{\frac{|\omega|}{2\pi}} \cdot \left| \frac{\varepsilon \tau}{(1+i\omega\tau)^{n+1}} \right|^2 \quad (35)$$

$$ENC_d^2 = \frac{d\varepsilon^2 \tau^2}{(2\pi)^{3/2}} \int_{-\infty}^{+\infty} d\omega \frac{\sqrt{|\omega|}}{(1+\omega^2 \tau^2)^{n+1}} \quad (36)$$

Substituting $x = \omega\tau$ and acknowledging that the function to be integrated is even, we can write:

$$ENC_d^2 = \frac{d\varepsilon^2 \sqrt{\tau}}{\pi} \sqrt{2\pi} \int_0^{+\infty} dx \frac{\sqrt{x}}{(1+x^2)^{n+1}}. \quad (37)$$

The final expression of the equivalent noise charge is thus:

$$ENC_d^2 = d \cdot (n!)^2 \left(\frac{e}{n} \right)^{2n} \frac{\sqrt{\tau}}{2\sqrt{\pi}} \cdot \eta_n \quad (38)$$

with

$$\Omega_4(n) = (n!)^2 \left(\frac{e}{n} \right)^{2n} \frac{1}{2\sqrt{\pi}} \cdot \eta_n \quad (39)$$

The parameter η_n varies according to the number of filter stages following the relation below:

$$\eta_n = \frac{\prod_{k=1}^n (4k-3)}{4^n n!} \quad (40)$$

The first five values for η_n are summarized in table I.

TABLE I
VALUES OF THE COEFFICIENT η_n FOR DIFFERENT VALUES OF n .

n	1	2	3	4	5
η_n	$\frac{1}{4}$	$\frac{5}{32}$	$\frac{15}{128}$	$\frac{195}{2048}$	$\frac{663}{8192}$

The reader may notice that, within this formalism, the value of ENC_d^2 seems to rise with the number of RC stages, which is counter-intuitive. This is due to the fact that keeping τ constant and increasing n the filter response function broadens. The peaking time is in fact equal to $n\tau$. We can use a better definition of the shaping time τ_s , considering the interval from the intercept with the time axis of the tangent at the inflection point of $s(t)$ to its peak:

$$\tau_s = (2\sqrt{n} - 1) \cdot \tau. \quad (41)$$

Re-writing (38) we obtain:

$$ENC_d^2 = d \cdot (n!)^2 \left(\frac{e}{n} \right)^{2n} \frac{\sqrt{\tau_s}}{2\sqrt{(2\sqrt{n}-1)\pi}} \cdot \eta_n \quad (42)$$

We can conclude that $ENC_d^2 = d\sqrt{\tau_s} \cdot k_n$ where the values of k_n are reported in table II.

TABLE II
VALUES OF THE COEFFICIENT k_n FOR DIFFERENT VALUES OF n .

n	1	2	3	4	5
k_n	0.5211	0.4449	0.4196	0.4063	0.3979

VI. CONSIDERATIONS ON THE COEFFICIENTS AND COMPARISON WITH OTHER ALREADY-KNOWN TERMS

Now that we have calculated the ENC coefficients for the parallel \sqrt{f} noise, we can evaluate its contribution in some typical cases. For sake of completeness, table III summarizes both in approximate and closed-form all the known noise coefficients.

Figures 2, 3 and 4 show the values of the weighting coefficients K_1 and K_4 reported in (13) for the white and colored noise components due to the resistor with distributed capacitance. Specifically, K_1 and K_4 are reported for different values of the ratio τ/τ_{RWD} , where τ is the filter shaping time and τ_{RWD} is defined in (3). More specifically, Fig. 2 shows the values of K_1 and K_4 for the trapezoidal shaping amplifier, Fig. 3 for the commercial Quasi-Gaussian shaping amplifier and Fig. 4 for the CR-RCⁿ shaping amplifier. The plotted functions are obtained integrating the expressions in (14) and (15) by means of numerical approximations.

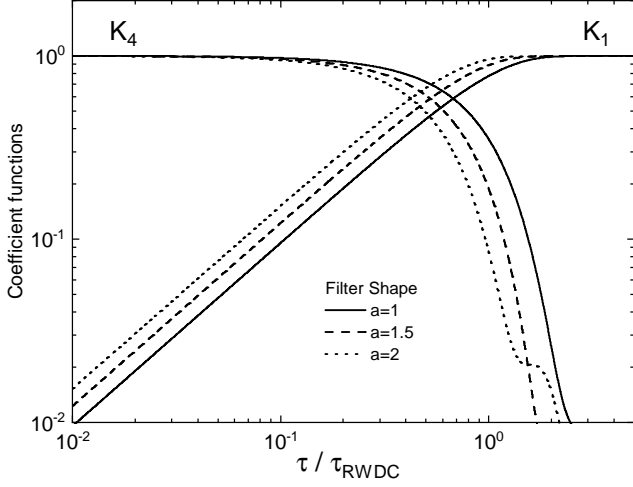


Fig. 2. Weighting coefficients K_1 and K_4 for a trapezoidal shaping amplifier with $\alpha=1$ (triangular shaping), 1.5 and 2.

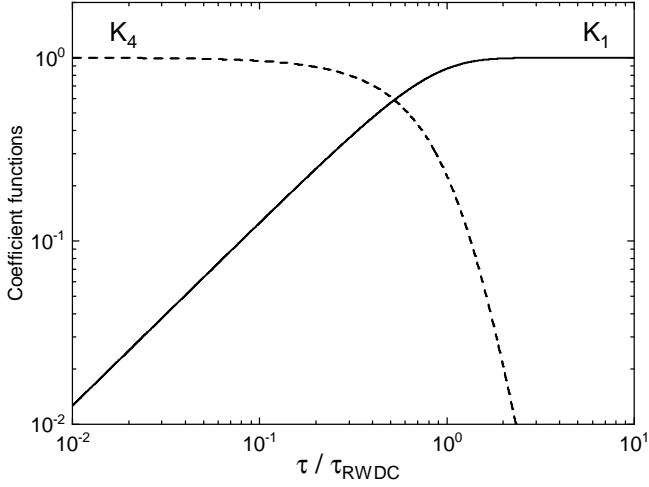


Fig. 3. Weighting coefficients K_1 and K_4 for a commercial 4th-order Quasi-Gaussian shaping amplifier.

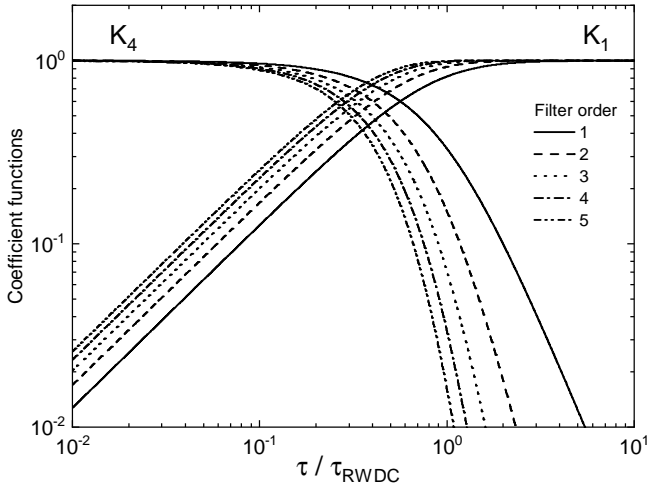











Fig. 4. Weighting coefficients K_1 and K_4 for a CR-RCⁿ shaping amplifier with $n=1,2,3,4,5$.

TABLE III
NOISE COEFFICIENTS SUMMARY TABLE. IT IS POSSIBLE TO CALCULATE THE EQUIVALENT NOISE CHARGE OF A SPECTROSCOPIC CHAIN USING (13). THE FUNCTION $f_1(\alpha)$ CAN BE CALCULATED IN CLOSED FORM AND CAN BE FOUND IN LITERATURE [14].

Filter type	Ω_1	Ω_2	Ω_3	Ω_4
Triangular/Trapez	$\alpha - \frac{1}{3}$	$f_1(\alpha)$	$\frac{1}{2\pi^2}$	$f_2(\alpha)$
$(\alpha = 1)$ 	(0.667)	(0.1405)	(0.05066)	(0.2813)
$(\alpha = 1.5)$ 	(1.167)	(0.1889)	(0.05066)	(0.4325)
$(\alpha = 2)$ 	(1.667)	(0.2200)	(0.05066)	(0.5559)
4-or QG 	2.025	0.1700	0.02362	0.5365
CR-RC 	$\frac{e^2}{4}$ (1.847)	$\frac{e^2}{(2\pi)^2}$ (0.1872)	$\frac{e^2}{4(2\pi)^2}$ (0.04679)	$\frac{e^2}{8\sqrt{\pi}}$ (0.5211)
CR-RC ² 	$\frac{3e^4}{64}$ (2.559)	$\frac{e^4}{8(2\pi)^2}$ (0.1729)	$\frac{e^4}{64(2\pi)^2}$ (0.02161)	$\frac{5e^4}{256\sqrt{\pi}}$ (0.6016)
CR-RC ³ 	$\frac{5e^6}{648}$ (3.113)	$\frac{4e^6}{243(2\pi)^2}$ (0.1682)	$\frac{e^6}{648(2\pi)^2}$ (0.01577)	$\frac{5e^6}{1728\sqrt{\pi}}$ (0.6586)
CR-RC ⁴ 	$\frac{315e^8}{2^{18}}$ (3.582)	$\frac{9e^8}{2^{12}(2\pi)^2}$ (0.16599)	$\frac{45e^8}{2^{18}(2\pi)^2}$ (0.01296)	$\frac{1755e^8}{2^{22}\sqrt{\pi}}$ (0.7037)
CR-RC ⁵ 	$\frac{567e^{10}}{8 \cdot 5^8}$ (3.996)	$\frac{24^2 e^{10}}{5^9(2\pi)^2}$ (0.1645)	$\frac{63e^{10}}{5^8 \cdot 8(2\pi)^2}$ (0.01125)	$\frac{5967e^{10}}{10^8\sqrt{\pi}}$ (0.7415)

$$f_1(\alpha) = \frac{1}{2\pi^2} [(\alpha-1)^2 \cdot \log(\alpha-1) + (\alpha+1)^2 \cdot \log(\alpha+1) - 2\alpha^2 \log(\alpha)]$$

$$f_2(\alpha) = \frac{8}{15\pi} [(\alpha-1)^{5/2} + (\alpha+1)^{5/2} - 2(1+\alpha^{5/2})]$$

VII. EXPERIMENTAL VERIFICATION

To verify the theoretical results obtained in the previous paragraphs, a 100 M Ω , 6 pF poly-silicon RWDC was used as feedback resistor of an integrated CSP (Charge Sensitive Pre-Amplifier) [12] with the fast-reset feature de-activated [15], [16], [17]. This pre-amplifier has been previously characterized [18] and shows a sufficiently low noise to allow for the measurement.

The first step was to connect only a discrete-type 100 M Ω feedback resistor to the CSP and perform the ENC measurement with no additional capacitance added to the input node. A pulse-generator was used to inject signals to the pre-amplifier

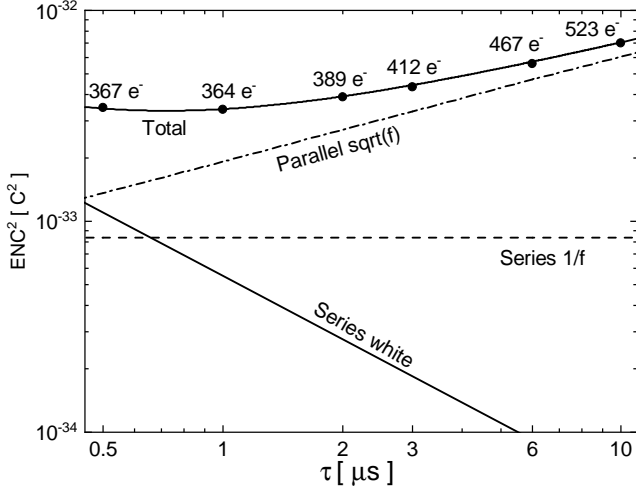


Fig. 5. Experimental values of ENC^2 obtained with the CSP equipped with integrated RWDC. On each of the black dots, representing the experimental data, labels are appended reporting the equivalent number of electrons r.m.s. The straight lines represent the ENC^2 different noise components, as obtained with the fitting algorithm.

and a Ortec 572 Spectroscopy Amplifier [13] was connected to its output. This first step allowed the measurement of the ratio ξ of the series white noise to the series 1/f noise. As a second step, the feedback discrete resistor was removed and the integrated 100 M Ω RWDC was connected to the same pre-amplifier. No other modifications on the set-up were made. The integrated RWDC is realized on an ASIC separated from the pre-amplifier and is packaged in a JLCC68 chip carrier. The connection of the RWDC in feedback to the pre-amplifier adds some capacitance to the input node of the CSP, which cannot be easily measured. The new ENC data were thus collected. Thanks to the previous measurement, the ξ ratio was inserted in the fitting algorithm in order to have a more accurate estimation of the series noise contribution. It appears that the connection of the RWDC adds a total of 1.5 pF to the input node, which is reasonable. The experimental ENC with the feedback RWDC in Fig. 5 shows a trend for long shaping times that clearly emphasizes the \sqrt{f} contribution. The contribution of the parallel white noise is not visible for the following two reasons. First, without a detector and using a p-MOS input transistor, both I_{DET} and I_{FET} of (7) are not present. Second, since the ratio τ/τ_{RWDC} is close to 10^{-3} in our case, $K1 \approx 10^{-3}$. On the other hand, the \sqrt{f} noise, that gives a ENC^2 contribution that is proportional to the square root of the shaping time, is clearly visible, since $K4 \approx 1$. The value of τ_{RWDC} was obtained by fitting the time-domain impulse-response function of the CSP, according to [6]. In order to give a statistical significance of the matching between the experimental data and the supposed $\sqrt{\tau}$ contribution, we can consider this as a counting measurement, where the number of electrons r.m.s. is accompanied by an error equal to the square root of such number. The χ^2 test made with 2 degrees of freedom (6 experimental data and 4 fitting parameters) gives a probability $P(\chi^2 > \chi_0^2) = 86\%$, that strongly confirms the hypothesis.

VIII. CONCLUSIONS

This paper calculates the ENC contribution of a feedback resistor with a high distributed capacitive coupling to a ground plane when used as feedback discharge device in a charge-sensitive pre-amplifier. Noise coefficients have been given as it is traditionally done in literature for standard noise components (series white, series 1/f, parallel white). It has been demonstrated that, since the RWDC noise is white for $f < f_{CORNER}$ and proportional to \sqrt{f} for $f > f_{CORNER}$, the total ENC contribution is a mixture of the one of a totally white noise and the one of a \sqrt{f} noise. The coefficients of this mixing depend on the ratio between $1/(2\pi f_{CORNER})$ and the filter shaping time. Experimental measurements of the ENC of a RWDC-equipped charge-sensitive pre-amplifier strongly confirm the theoretical model. Future works may address the interesting consequences of the Boella effect [19] on the RWDC noise, ultimately limiting the increase of its PSD at high frequency.

REFERENCES

- [1] M. Assié *et al.*, “New methods to identify low energy ^3He with silicon-based detectors,” *Nucl. Instrum. Methods A*, vol. 908, p. 250 – 255, 2018. doi: 10.1016/j.nima.2018.08.050
- [2] S. Capra *et al.*, “Performance of the new integrated front-end electronics of the TRACE array commissioned with an early silicon detector prototype,” *Nucl. Instrum. Methods A*, vol. 935, pp. 178–184, 2019. doi: 10.1016/j.nima.2019.05.039
- [3] N. D. Marco, “Searching for neutrinoless double-beta decay with GERDA,” *Nucl. Instrum. Methods A*, 2019. doi: https://doi.org/10.1016/j.nima.2019.04.066
- [4] W. Buttler, B. Hosticka, and G. Lutz, “Noise filtering for readout electronics,” *Nucl. Instrum. Methods A*, vol. 288, no. 1, pp. 187–190, 1990. doi: 10.1016/0168-9002(90)90484-N
- [5] E. Gatti and P. Manfredi, “Processing the signals from solid-state detectors in elementary-particle physics,” *La rivista del nuovo cimento* 1978-1999, 1986. doi: 10.1007/BF02822156
- [6] S. Capra, “Impedance and noise closed-form model of large-area integrated resistors with high stray capacitance to be used as feedback discharge devices in charge-sensitive preamplifiers for nuclear spectroscopy,” *IEEE Trans. Nucl. Sci.*, vol. 67, no. 4, pp. 722–731, 2020. doi: 10.1109/TNS.2020.2975311
- [7] S. Capra and A. Pullia, “Study of the effects of parasitic capacitance on large integrated feedback resistors for charge-sensitive preamplifiers,” 2014 *IEEE NSS/MIC conf. rec.*, 2016. doi: 10.1109/NSS-MIC.2014.7431042
- [8] —, “Measurement of the power spectral density of noise produced by a large integrated feedback resistor for charge-sensitive preamplifiers,” 2016 *IEEE NSS/MIC conf. rec.*, vol. 2017-January, 2017. doi: 10.1109/NSSMIC.2016.8069661
- [9] S. Capra, D. Mengoni, R. Aliaga, A. Gadea, V. Gonzalez, and A. Pullia, “Design of an integrated low-noise, low-power charge sensitive preamplifier for γ and particle spectroscopy with solid state detectors,” 2014 *IEEE NSS/MIC conf. rec.*, 2016. doi: 10.1109/NSSMIC.2014.7431043
- [10] F. Mele, M. Gandola, and G. Bertuccio, “Sirio: A high-speed CMOS charge-sensitive amplifier for high-energy-resolution x-gamma ray spectroscopy with semiconductor detectors,” *IEEE Trans. Nucl. Sci.*, vol. 68, no. 3, pp. 379–383, 2021. doi: 10.1109/TNS.2021.3055934
- [11] A. Castoldi, C. Guazzoni, and T. Parsani, “Versatile multi-channel CMOS frontend with selectable full-scale dynamics from 100 MeV up to 2.2 GeV for the readout of detector’s signals in nuclear physics experiments,” *Nuovo Cimento della Società Italiana di Fisica C*, vol. 41, no. 5, 2018. doi: 10.1393/ncc/i2018-18168-6
- [12] S. Capra and A. Pullia, “Design and experimental validation of an integrated multichannel charge amplifier for solid-state detectors with innovative spectroscopic range booster,” *IEEE Trans. Nucl. Sci.*, vol. 67, no. 8, pp. 1877–1884, 2020. doi: 10.1109/TNS.2020.3006892
- [13] “Ortec 572a amplifier, accessed Aug. 2022.” [Online]. Available: https://www.ortec-online.com/products/electronics/amplifiers/572a

- [14] V. Radeka, *Signal Processing for Particle Detectors: Datasheet from Landolt-Börnstein - Group I Elementary Particles, Nuclei and Atoms · Volume 21B1: "Detectors for Particles and Radiation. Part 1: Principles and Methods"* in *SpringerMaterials*, C. W. Fabjan and H. Schopper, Eds. Springer-Verlag Berlin Heidelberg.
- [15] S. Capra, G. Secci, and A. Pullia, "An innovative analog circuit to retrieve energy information from signals of deeply saturated preamplifiers connected to semiconductor detectors," *IEEE Trans. Nucl. Sci.*, vol. 69, no. 7, p. 1757 – 1764, 2022. doi: 10.1109/TNS.2022.3178760
- [16] A. Pullia and S. Capra, "Experimental performance of a highly-innovative low-noise charge-sensitive preamplifier with integrated range-booster," *Journal of Instrumentation*, vol. 13, no. 12, 2018. doi: 10.1088/1748-0221/13/12/C12004
- [17] A. Pullia, F. Zocca, and S. Capra, "Note: A 102 db dynamic-range charge-sampling readout for ionizing particle/radiation detectors based on an application-specific integrated circuit (ASIC)," *Review of Scientific Instruments*, vol. 89, no. 2, 2018. doi: 10.1063/1.5012081
- [18] S. Capra, R. Aliaga, D. Mengoni, P. John, A. Gadea, V. Herrero, and A. Pullia, "Evaluation of the spectroscopic performance of the integrated multi-channel charge-sensitive preamplifier of TRACE with a silicon detector prototype," *2016 IEEE NSS/MIC conf. rec.*, vol. 2017-January, 2017, doi: 10.1109/NSSMIC.2016.8069657
- [19] M. Boella, "Sul comportamento alle alte frequenze di alcuni tipi di resistenze in uso nei radiocircuiti (On the high frequencies behavior of some types of resistors used in radio circuits)," *Alta Frequenza*, vol. 3, pp. 132–148, 1934.